Chemical Engineering Journal 106 (2005) 241–247

Chemical Engineering Journal

www.elsevier.com/locate/cej

On the use of a non-thermal plasma reactor for ethanol steam reforming

O. Aubry*, C. Met, A. Khacef, J.M. Cormier

GREMI-Polytech'Orléans, 14 rue d'Issoudun, B.P. 6744, 45067 Orléans Cedex 2, France

Received 21 July 2004; received in revised form 28 October 2004; accepted 4 December 2004

Abstract

This work is dedicated to the steam reforming study of ethanol in a non-thermal plasma reactor at low temperature and at atmospheric pressure. The plasma reactor was powered by a high voltage 50 Hz AC power supply with a 155 mA sinusoidal current. The voltage delivered by this system was self-adjusted between 0.4 and 1 kV according to the primary voltage of the transformer. Outlet concentration species, mainly H_2, CO and CO_2, were determined using chemical analysis apparatus and studied as functions of the electrical power and electrical discharge characteristics. Reactor behaviour and plasma product distribution are strongly determined by the electrical power and ethanol/water ratio. Chemical species and physical parameter variations have been described using two overall reactions: the ethanol steam reforming and endothermic cracking reactions. This present paper shows interesting results in comparison with catalytic processing of ethanol steam reforming.

Keywords: Hydrogen; Non-thermal plasma; Steam reforming; Ethanol

1. Introduction

Fuel cells are considered as a clean energy source. Nevertheless, since hydrogen is difficult to transport and store, its production in situ from an easily transported liquid feedstock can be an efficient alternative. The use of ethanol for energy production is an effective solution for the reduction of CO_2 emissions and preserves the fossil energy resources. Taking these aspects into consideration, the bio-ethanol steam reforming seems to be a promising technique [1,2]. Ethanol can be obtained by fermentation of surplus or agricultural residues and therefore is a renewable energy source that can be used to the H_2 production. During last decade, studies showed that hydrogen present a potential use as a fuel for electricity generation and transportation purposes. Moreover, H_2 is a renewable energy source and do not contribute to the green house effect [3,4]. The use of ethanol catalytic reactors for H_2 production had been presented in previous studies [1,2,5–8]. Nevertheless, some authors have performed the possibility to use plasma reactors for the hydrogen production from water and hydrocarbons [9–12].

The aim of the present paper is to study the steam-reforming from ethanol with a non-thermal plasma reactor to perform chemical analysis of the exhausts gas by micro gas chromatography (μGC) and Fourier transform infrared techniques (FTIR) and to identify the main ways implicated.

2. Experimental

The experiments were conducted at atmospheric pressure with a liquid ethanol/water mixture heated by graphite electrodes in a plasma reactor. The electrode gap was 10 mm. The length and diameter of the electrode were 150 and 25 mm, respectively. Fig. 1 is a schematic representation of the experimental reactor. The ethanol and water mole fractions ratio of the inlet mixture studied was in the range from 0–0.72.

* Corresponding author. Tel.: +33 238 494609; fax: +33 238 417154.
E-mail address: olivier.aubry@univ-orleans.fr (O. Aubry).

1385-8947/$ – see front matter © 2004 Elsevier B.V. All rights reserved.
doi:10.1016/j.cej.2004.12.003

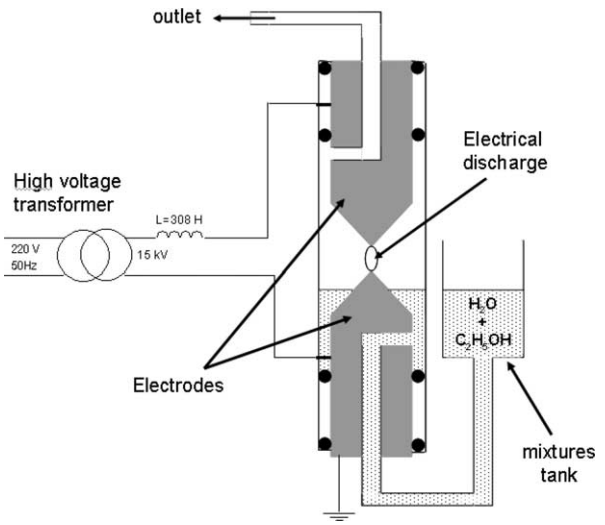

Fig. 1. Schematic reactor experimental.

The outlet gas composition was analysed using two techniques: micro gas chromatography (μGC, Varian CP2003-P) and Fourier transform infra-red (FTIR, Nicolet Magna-IR 550 series II). The μGC analyser contained 5 Å Molecular sielve and Plot Q columns. Both columns were equipped with thermal conductivity detectors (TCD) calibrated with standards of known composition. The temperatures of the column and injector for the analysis of H_2, CH_4 and CO on the Molecular sielve 5 Å column were 70 and 85 °C for Poraplot Q and the analysis of hydrocarbons and CO_2. The 10 m long FTIR analysis cell was maintained at 110 °C. The species detected and analyzed were H_2, CH_4, C_2H_2, C_2H_4, C_2H_6, CO, CO_2, C_2H_5OH and H_2O. The latter two were detected only in humid gas. The H_2O concentration at reactor output was estimated from the C, H and O balances, since no other specie was detected in our work.

The exhaust gas was sampled through a hole, in the second electrode, which was linked to μGC via a heating pipe (110 °C) to quantify the moisture gas or via the heating pipe until a cryogenic trap (−30 °C) to analyse the desiccated gas.

The current and voltage waveforms were measured using a TCP202 Tektronix Hall effect probe and a P5205 Tektronix high voltage differential probe connected to a voltage divider with a ratio of 0.01. The signals from the probes were recorded on a Tektronix TDS 460A digital oscilloscope and processed in a PC.

The gas discharge power was determined from voltage and current measurements. The electrical discharge was powered by a 50 Hz high voltage step-up transformer with leakage flux (AUPEM SEFLI high voltage transformer: primary 230 V, 10000/100, I_2 = 155 mA). The sinusoidal current remains at a constant value of 155 mA. In order to verify the running stability, several voltage and current recording were performed for each liquid mixture. Finally, the signal processing was performed on a PC.

3. Results

3.1. Chemical analysis

3.1.1. Dry gas

The dessicated gas mole fractions as functions of the inlet mole fractions ratio are displayed Fig. 2. FTIR and μGC were associated in this study. The species detected were: H_2, CO, CO_2, CH_4 and C_2 hydrocarbons. No reactive species (C_2H_5OH and H_2O) were detected with the use of the cryogenic trap.

As the inlet ethanol/water ratio rises, the mole fractions of H_2 and CO_2 decrease, from 0.72 to 0.62 and from 0.10 to 0.013, respectively. The concentration of the others species

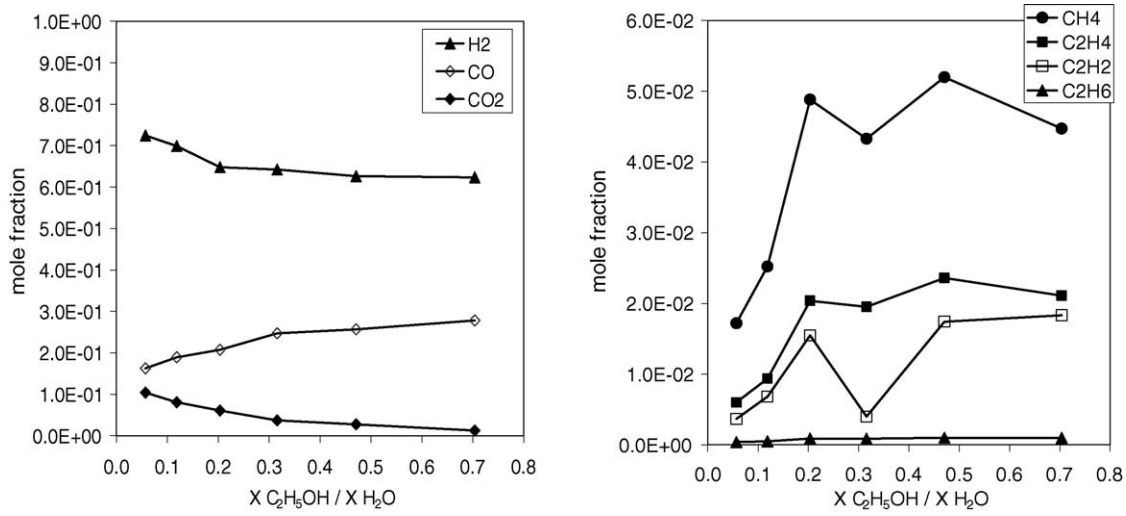

Fig. 2. Composition of the dried exhaust gas vs. the inlet ethanol/water ratio.

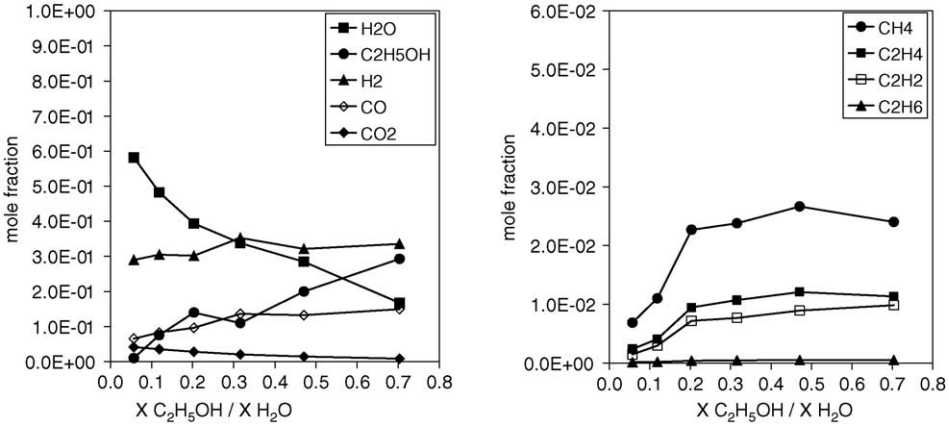

Fig. 3. Composition of the wet exhaust gas vs. the inlet ethanol/water ratio.

increase: CO mole fraction rises from 0.16 to 0.28 and the concentration of the hydrocarbons species stays below 0.05 in the entire studied domain.

3.1.2. Wet gas

The study of dry gases does not enable all species present at reactor output to be quantified. Indeed, to analyse all the products and especially the no-consumed species (H_2O and C_2H_5OH), we have studied the wet exhaust gas composition. Mole fractions of these species are presented in Fig. 3 as functions of the inlet mole fractions ratio.

H_2 concentration slightly increases from 0.29 to 0.34 when the ethanol/water ratio rises. Simultaneously, the mole fractions of CO, CH_4, C_2H_2, C_2H_4 and C_2H_6 rise from 0.06 to 0.15, 6.8×10^{-3} to 2.4×10^{-2}, 2.4×10^{-3} to 1.14×10^{-2}, 1.46×10^{-3} to 9.86×10^{-3} and 1.56×10^{-4} to 5.32×10^{-4}, respectively. The CO_2 decreases from 4.16×10^{-2} to 8.74×10^{-3}.

Trends in mole fractions variations for the others species are similar to the dried gas results. Low concentrations of hydrocarbons are observed in the outlet gas.

Our dry results show that there were high mole fractions of H_2 at reactor output, of the order of 0.6 to 0.7. In order to carry out the complete energy balance involved in this process, however, it is necessary to take into account all species present at reactor output, i.e. wet gas. Dry and wet gas comparisons of no-condensed species show that the mole fractions in the wet outlet gas are nearly divided by 2. In the wet case, the concentrations of H_2, CO, CO_2, CH_4 and of C_2 compounds decreased because H_2O and C_2H_5OH were included in the quantification of species at reactor output. This shows that it is important to take all species present and not only dry gases into account, in order to establish a complete material and energy balance in this type of process. Moreover, the precursors (C_3, C_4) of aromatic or polyaromatic species that lead to the formation of soot are absent, explaining the absence of carbon deposit.

C_2H_5OH and H_2O are not fully converted. The corresponding conversion rates, τ, are defined by the following expression:

$$\tau = \frac{n_{\text{cons}}}{n_{\text{i}}} \quad (1)$$

where n_{cons} represents the consumed number of moles of each reactant and n_{i} is the number of moles of inlet reactant. Results are shown in Table 1. Conversion rates depend on the inlet ethanol/water ratio. Ethanol conversion decreases and water conversion increases when C_2H_5OH/H_2O ratio rises.

Table 1
Examples of C_2H_5OH and H_2O conversion rates

Inlet XC_2H_5OH/XH_2O	0.12	0.32	0.70
τ C_2H_5OH	0.39	0.27	0.22
τ H_2O	0.15	0.23	0.36

3.2. Characteristics of the discharge

Fig. 4 shows the variations of the voltage and current as functions of the time for a given liquid mixture: ethanol/water ratio = 0.12.

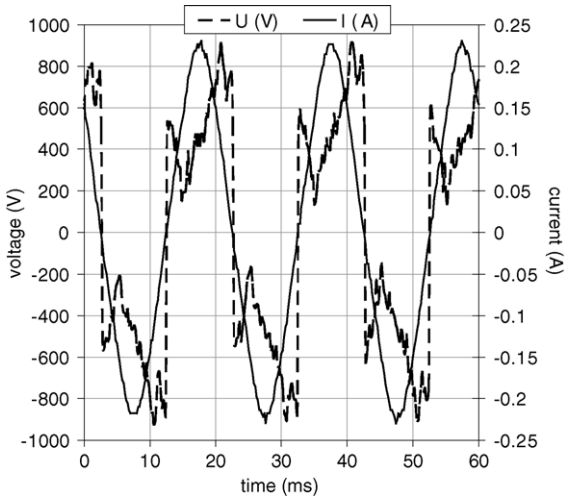

Fig. 4. Variation of the voltage and current as functions of the time. Ethanol/water = 0.12.

The plasma reactor is powered by a 50 Hz step-up transformer. Root mean square (RMS) value of the sinusoidal current is 155 mA. The secondary voltage applied to the discharge gap is self-adjusted as an effect of leakage flux in the range: 0.4–1.0 kV. Periodic ignition of the discharge is corresponding to a voltage pulse. The ignition pulses magnitude values are in the range 400–500 V. A characteristic parameter of the plasma was determined, corresponding approximately to the maximum degree of ionization, by measuring the resistance value of the ionized column when current is maximal. This value in a steam plasma is 1600 Ω when the length of the ionized column is 15 mm. The voltage drop at the electrodes is 60 V. The instantaneous discharge resistance changes with time during each half-period of current.

As the plasma is recombining the resistance is increasing and greatest voltage values are observed for a corresponding time of about 10 ms. Pulses magnitude and maximum voltages are linked to the inlet ethanol/water ratio.

Fig. 4 shows voltage and current variations of the plasma discharge. Ignition values and maximum of voltage can be observed. Due to the leakage flux effect, a large inductance appears and the current remains at a nearly constant RMS value of 155 mA with a sinusoidal waveform. Voltage is determined by ionization properties of the gaseous mixture. Previous studies [13–15] had shown a non-thermal plasma behaviour in which electrons temperature (8000–1000 K) is higher than the gas temperature. Plasma column looks like a plasma string with 1 and 10 mm for diameter and length, respectively. The order of magnitude of the maximum gas temperature is 2000 K and the average temperature at the reactor outlet is about 600 K. In light of the voltage drop at the electrodes and of the temperature difference between electrons and the gas, it can be said that the discharge is a "glow discharge", illustrating the non-thermal nature of the plasma.

In the case of Fig. 4, the average power provided to plasma discharge is about 66 W. A non-linear behaviour of the plasma discharge can be observed. This non-linear effect is shown in Figs. 4 and 5.

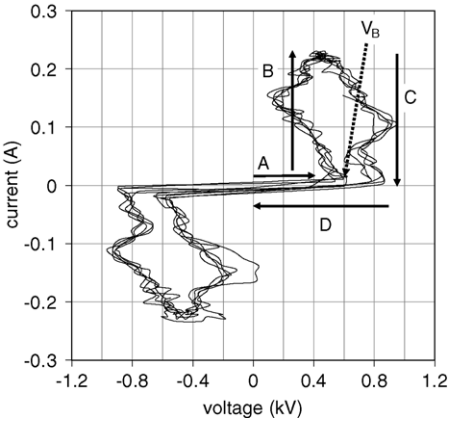

Fig. 5. Dynamical current–voltage characteristic. Ethanol/water = 0.12.

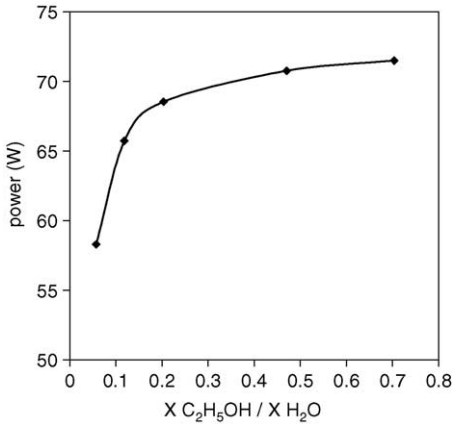

Fig. 6. Power of the discharge vs. the inlet composition.

Fig. 5 shows four phases are observed corresponding to the following effects:

(A) increasing voltage without significant current;
(B) full ionisation region corresponding to current increasing;
(C) recombination region with increasing of the plasma column resistance;
(D) weak ionisation region.

Transition from A to B is characterized by a breakdown potential V_B (ignition of the discharge). This potential is a function of the gas mixture. V_B is increasing as the C_2H_5OH concentration increases.

The input electrical discharge power, P_i, is calculated from voltage and current measured for each mixture: $P_i = \frac{1}{T}\int_o^T u_{(t)} i_{(t)}\,dt$; with $u_{(t)}$ and $i_{(t)}$ voltage and current, respectively.

As shown in Fig. 6, P_i strongly depends on the inlet composition. P_i rapidly increases from 57 to 69 W when the inlet ethanol/water mole fractions ratio rises from 0.05 to 0.20. Above this upper limit, the input power slightly increases up to 72 W. This means that the voltage is linked to the inlet composition because of a constant value of the current. Therefore, the average voltage increases when the input power rises.

4. Interpretation and energy balance

The fine interpretation of the reaction mechanisms involved in this type of reactor requires the use of a kinetic model coupled with a hydrodynamic model of the plasma that includes electron reactions. This study is complex and requires the participation of specific high level competence. Our current understanding does not enable us to present the comparison between a model and local measurements of the density of different species. Taking the context into account, we present only the overall experimental results, describing the principal parameters of system advancement. So, to estimate the energy balance, we represented the chemical

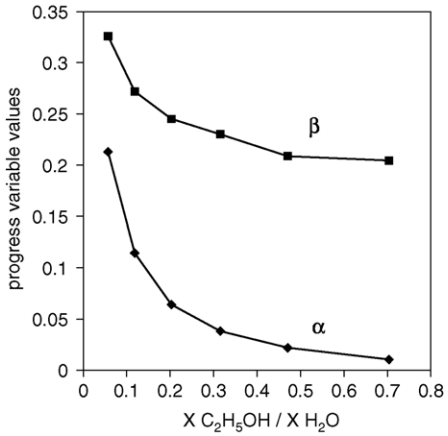

Fig. 7. Conversion degree of the overall reactions Eqs. (2) and (3).

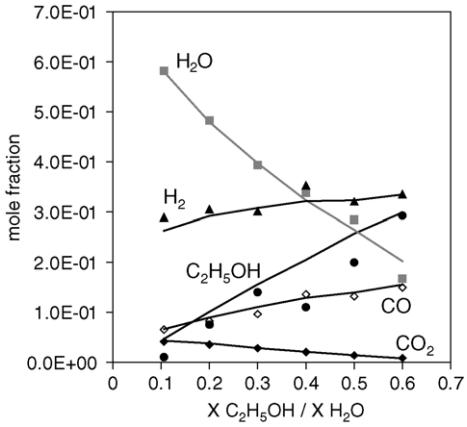

Fig. 8. Experimental mole fractions (symbols) and calculated values (solid lines) vs. the inlet composition.

system from two global reactions. Indeed, from our experimental data, the general evolution observed for the main species in the wet gas could be described by considering two overall reactions:

$$C_2H_5OH + 3H_2O \rightarrow 2CO_2 + 6H_2 \quad (2)$$

$$C_2H_5OH + H_2O \rightarrow 2CO + 4H_2 \quad (3)$$

For each C_2H_5OH–H_2O mixture, H_2, CO, CO_2, C_2H_5OH and H_2O mole fractions can be expressed in terms of the progress variables α, β of reactions (2) and (3). A least square procedure has been used to derive α and β values to minimize the sum $\sum (Xi_{exp} - Xi_{calc})^2$. In order to calculate the relative importance of the two global reactions representing changes of major species (H_2, CO, CO_2, C_2H_5OH, H_2O) and to calculate the energy involved in the chemical process, we determined the consumption of reactants in the two reactions. We calculated the mole fractions of species, noted Xi_{calc}, versus the progress values (α and β) of the two reactions (2) and (3). This provides the lowest sum $\sum (Xi_{exp} - Xi_{calc})^2$ for each reaction mixture. The Xi_{exp} values are the mole fractions measured of the species analyzed. The results are shown in Fig. 7.

α decreases down to 0 and β decreases to a stable value (0.22) for the highest ethanol mole fraction. This latter explains the nearly constant H_2, CO and CO_2 mole fractions. H_2O and C_2H_5OH are consumed by these reactions. For the lowest inlet ethanol mole fraction, the consumption of ethanol occurs by reactions (2) and (3) in same part and contribute to form H_2.

When inlet C_2H_5OH mole fraction increases, reaction (3) dominates the consumption of ethanol which explains the lowest CO_2 mole fractions in favour of the CO production.

The experimental mole fractions are compared with the mole fractions calculated from the progress variables (Fig. 8). The results in Fig. 8 show that the description using two reactions mentioned above, combined with α and β, is sufficient for an overall description of the effect of the plasma. We can thus use these degrees of advancement to calculate an energy balance.

By taking into account the progress variables of the two overall reactions, power balance of the reactor can be performed. Fig. 9 displays different powers: input power, P_i, power used to vaporize the inlet mixture, P_v, and power implied in the two overall chemical reactions, P_r.

The vaporization power, P_v, is calculated from the liquid volume consumed, ethanol and water vaporization enthalpies (−42.3 and −44 kJ mol^{-1}) and the inlet mole fraction of ethanol. The vaporization power calculated is in the range from 58 to 72 W when ethanol/water ratio increases from 0.05 to 0.72.

Previous studies showed that theses electrical discharges imply low electron densities, high electron temperature and low gas temperature. We assumed a maximum gas temperature in the plasma column of about 2000 K [13–15]. The enthalpies of the overall reactions (2) and (3) were calculated at 2000 K: $\Delta_r H_2$ and $\Delta_r H_3$ are 220.05 and 272.1 kJ mol^{-1}, respectively.

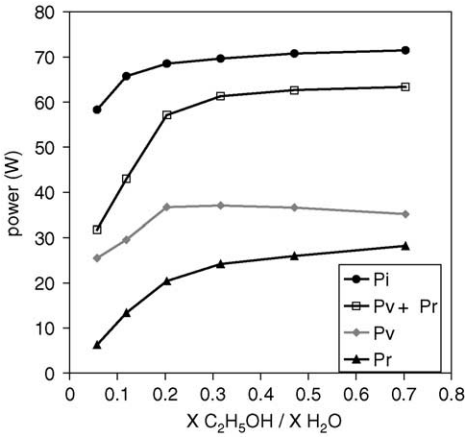

Fig. 9. Input, vaporization, reaction and vaporization + reaction powers vs. ethanol/water ratio.

Thus, the overall enthalpy in the reactions is expressed by the equation (4):

$$\Delta_r H = \alpha \Delta_r H_1 + \beta \Delta_r H_2 \quad (4)$$

α and β are the progress values obtained previously (Fig. 7).

From $\Delta_r H$ calculated, the power used in the chemical reactions, P_r, can be estimated. P_r is a function of the inlet ethanol mole fraction. This power is in the range from 6 to 28 W.

Our results showed that the vaporization of the ethanol/water mixtures require more energy than that implied in the chemical process. These powers are strongly influenced by the composition of the inlet mixture. As lowest ethanol/water ratio, the power implicated in the hydrogen production is decreasing. If we compare input power and the sum of P_v and P_r as functions of inlet ratio, we can observe that $P_v + P_r$ is close to P_i when the inlet ethanol/water ratio is above 0.2. As it is shown in Fig. 9, main part of the input power is used to the vaporisation and chemical reactions.

A dramatic influence of the inlet mixture was observed in input power and applied voltage. The rise of the ethanol/water ratio leads to an increase of the electric resistance in the ionized gas phase. Moreover, the ionized gas phase composition in the electric discharge is an important factor on plasma and gas phase temperatures. Electron densities and temperatures depend on the inlet parameters and electrical properties. Thus, an increase of the hydrocarbon species concentration can lead to a decrease of these temperatures. Therefore, the decrease of the electrical resistance of the ionized gas phase can be understood.

A comparison between the results of this plasma steam reforming and catalytic steam reforming appears to be interesting.

Nevertheless, it is very difficult to find in the literature results on the concentrations of the species produced in wet gases. Therefore, Table 2 presents the mole fractions of main species present in the dry gas in different ethanol steam reforming processes.

The catalytic and non-thermal plasma results show a same order of magnitude for H_2, CO, CO_2 and CH_4 concentrations. We observe that plasma technology allows to achieve a good level of H_2 mole fraction in a great range of ethanol/water ratio comparing to the catalytic techniques. Llorca et al. [5] obtained gas exhaust without CO in the case of Co/ZnO catalysts while plasma method implies relative high CO mole fractions. The others species present same concentration levels.

Table 2
Comparative H_2, CO, CO_2, CH_4 mole fractions in the dry outlet gas vs. inlet ethanol/water ratio and vs. steam reforming techniques used

	This work	Auprêtre et al. [1]	Llorca et al. [5]
Inlet ethanol/water ratio	0.05–0.72	0.33	0.07
H_2	0.62–0.72	0.44–0.72	0.65–0.738
CO	0.16–0.28	0.07–0.20	–
CO_2	0.10–0.12	0–0.21	0.216–0.242
CH_4	0.017–0.052	0–0.21	0.003–0.008

This comparison indicates that plasma steam reforming of the ethanol is a competitive way to produce H_2 with CO and CO_2. Nevertheless, the CO concentration is the main drawback because of concentrations higher than 10 ppm. This value is considered as a limit in order to avoid poisoning fuel cells.

5. Conclusions

This work shows that non-thermal plasma steam reforming of the ethanol at atmospheric pressure is a promising technique for H_2 production. Our results are very close to ones obtained in the catalytic reactors.

Chemical analysis of the outlet gas and characteristics of the discharge had been studied. We quantified the wet and dry exhaust gas composition. Thus, several species had been quantified: no-consumed reactive species (C_2H_5OH and H_2O), oxygenated, and hydrocarbon products (H_2, CO, CO_2, CH_4, C_2H_2, C_2H_4, C_2H_6). The mole fractions of CO and CO_2 depended on the inlet composition while H_2 concentrations remained constant. These results showed that the optimization of the process was important to reduce the CO mole fraction. Indeed CO was poisoning specie for the fuel cells; its concentration must be limited near 10 ppm. Chemical interpretation of the results in term of two overall reactions showed that parallel reactions could describe the conversion of the inlet ethanol and water. For the lowest inlet ethanol mole fractions, the progress variable values were in the same order of magnitude. For the highest ethanol mole fraction, the reaction leading to the CO_2 production becomes negligible. The method for producing hydrogen from ethanol with the plasma reactor described here is interesting and could, after additional work and depending on the results obtained, be developed at the industrial scale. Compared to conventional techniques, its principal advantages would be ease of use and uncomplicated control of the various operating parameters. We can envision the regulation of gas flows by adding auxiliary heating, combined with a command suited to the power delivered by the plasma. In addition, the plasma system eliminates problems related to the use of catalysts prepared from costly materials (Pt, Rh, Ru, Co, ...) and that require precautions in use and operation in order to optimize conversion rates and avoid the inactivation of catalysts by poisoning. The energy balances show that it is possible to reach yields very close to those calculated from the laws of thermodynamics. These balances carried out with a laboratory scale reactor are a determinant element that should arouse the interest of industries concerned in order to continue investigations on the possible applications of this technology.

The non-thermal plasma appears as a good technique for the steam reforming from bio-ethanol with a high H_2 concentration. Energetic costs could be decreased by re-injecting

the condensed gas phase containing water and ethanol. Moreover, to achieve low CO mole fractions, studies on others inlet mixtures with hydrocarbon-ethanol and/or a plasma-catalysis technique can be envisaged.

References

[1] F. Auprêtre, C. Decorme, D. Duprez, Catal. Commun. 3 (2002) 263–267.
[2] G.A. Deluga, J.R. Salge, L.D. Schmidt, X.E. Verykios, Science 303 (2004) 993–997.
[3] J. Benemann, Nat. Biotechnol. 14 (9) (1996) 1101–1103.
[4] J.-J. Lay, Y.-J. Lee, T. Noike, Water Res. 33 (11) (1999) 2579–2586.
[5] J. Llorca, N. Homs, J. Sales, P. Ramirez de la Piscina, J. Catal. 209 (2002) 306–317.
[6] J.P. Breen, R. Burch, H.M. Coleman, Appl. Catal. B: Environ. 39 (2002) 65–74.
[7] F.J. Marino, E.G. Cerrella, S. Duhalde, M. Jobbagy, M.A. Laborde, Int. J. Hyd. Energy 23 (12) (1998) 1001–1095.
[8] E.Y. Garcia, M.A. Laborde, Int. J. Hyd. Energy 16 (5) (1991) 307–312.
[9] J.M. Cormier, I. Rusu, J. Phys. D: Appl. Phys. 34 (2001) 2798–2803.
[10] F.N. Pekhota, V.D. Rusanov, S.P. Malyshenko, Int. J. Hyd. Energy 23 (10) (1998) 967–970.
[11] K. Meguernes, J. Chapelle, A. Czernichowski, J. High Temp. Mater. Proc. 5 (3) (2001) 363–374.
[12] A. Huang, G. Xia, J. Wang, S.L. Suib, Y. Hayashi, H. Matsumoto, J. Catal. 189 (2000) 349–359.
[13] A. Kaminska, J.-M. Cormier, S. Pellerin, O. Martinie, J. High Temp. Mater. Proc. 5 (3) (2001) 403–409.
[14] S. Pellerin, J.-M. Cormier, F. Richard, K. Musiol, J. Chapelle, J. Phys. D 32 (1999) 891–897.
[15] J.M. Cormier, I. Rusu, A. Kaminska, J. High Temp. Mater. Proc. 6 (4) (2002) 421–429.